CHEMICAL ENGINEERING TRANSACTIONS
VOL. 91, 2022
A publication of AIDIC
The Italian Association of Chemical Engineering
Online at www.cetjournal.it
Guest Editors: Valerio Cozzani, Bruno Fabiano, Genserik Reniers

ISBN 978-88-95608-89-1; ISSN 2283-9216
DOI: 10.3303/CET2291099

Methylene Blue Removal Using Palm Oil Mill Effluent Sludge-Derived Adsorbent

Farah Amelia Shahirah Roslan, Noorfidza Yub Harun*, Anwar Ameen Hezam Saeed, Raihan Mahirah Ramli, Sharvinaa Devi Mannikam, Ebrahim Hamid Hussein Al-Qadami

Department of Chemical Engineering, Universiti Teknologi PETRONAS (UTP), 32610 Bandar Seri Iskandar, Perak Darul Ridzuan, Malaysia
noorfidza.yub@utp.edu.my

Textile industries release a large amount of dye effluent into the wastewater that can cause health issues and endanger aquatic animals. In this study, sludge derived biochar (SB) adsorbent was produced from sewage sludge to remove methylene blue (MB) dye from wastewater. The surface area and porosity of SB are analysed by using Field Emission Scanning Electron Microscope (FESEM) and Surface Area and Pore analyser (SAP). The factors that affect the adsorption of MB in aqueous solution with SB adsorbent in batch mode are adsorbent dosage (0.5g, 1g), initial MB concentration (50 – 250 mg/L), and contact time (0 – 120 minutes). The Langmuir isotherm model fits the adsorption equilibrium results, and the pseudo-second-order kinetic model best describes the sorption kinetics of MB. The maximum adsorption capacity of MB decreases from 15.37 mg/g to 8.61 mg/g as the adsorbent dosage increases from 0.5 g to 1.0 g and contact time increases from 45 minutes to 60 minutes. Hence, sludge derived biochar is an effective adsorbent for the removal of MB dye from wastewater.

1. Introduction

The synthetic origin of industrial dyes has a high concentration of suspended solids, aromatic pollutants, alkaline properties, chemical oxygen demand, and biochemical oxygen demand in wastewater. The defiant nature of dyes possesses a threat to the environment and also to human health such as hypertension, fever, and mental disorder (Chaukura et al., 2017; Fan et al., 2017). The methylene blue (MB) dye referred to in this study is discharged in the lake and river (Saeed et al., 2019). Moreover, MB cannot be removed by conventional treatment systems such as advanced chemical oxidation technology, membrane treatment, and photo-degradation due to its high solubility and non-degradable nature (Chaukura et al., 2017; Fan et al., 2017). The adsorption method favours MB removal due to its low cost, high efficiency, and easy operational system. Activated carbon is an effective adsorbent for the adsorption process, but it comes with a high capital cost for small-scale applications (Sajab et al., 2010). Therefore, low-cost, green and efficient adsorbent from biomass such as sludge has demonstrated outstanding MB removal capability from wastewater compared to activated carbon (Otero et al., 2003). Sludge is the by-products of wastewater treatment plants (Otero et al., 2003). The process of upcycling the sludge waste into adsorbent can reduce the pollutants in the environment while removing MB from wastewater with a lower adsorbent material cost. SB is prepared at a lower temperature than commercial activated carbon, which shows that SB is cheaper than activated carbon (Chaukura et al., 2017; Fan et al., 2017). In general, the adsorption capacity is determined by the chemical structure and the porous structure of the adsorbent, which leads to alternative models for adsorption capacity based on the adsorption from cationic and anionic solution adsorbate (Saeed et al., 2020). Biochar as an adsorbent has recently gained attention, especially the ones derived from agricultural residues like rice husk (Saeed et al. 2021a), Kenaf (Saeed et al. 2021b), coconut coir (Paranavithana et al. 2016), sawdust (Mashkoor and Nasar, 2020), corn straws (Lian et al., 2016), pineapple bark (Guo et al., 2018), durian husk (Ahmad et al., 2015), hickory wood (Ding et al. 2016), and tea waste (Vithanage et al., 2016). Biochar is

Paper Received: 11 February 2022; Revised: 8 April 2022; Accepted: 11 May 2022
Please cite this article as: Roslan F.A.S., Yub Harun N., Saeed A.A.H., Ramli R.M., Mannikam S.D., Hussein Al-Qadami E.H., 2022, Methylene Blue Removal Using Palm Oil Mill Effluent Sludge-derived Adsorbent, Chemical Engineering Transactions, 91, 589-594 DOI:10.3303/CET2291099

effective, affordable and environmentally friendly adsorbent material for dye removal from wastewater (Saeed et al., 2018, Saeed et al., 2020). Therefore, the study aims to study the adsorption performance of biochar using sludge from wastewater treatment plants by evaluating the initial concentration, adsorbent dosage and the contact time that affects the removal of MB through adsorption.

2. Methodology

2.1 Sample pre-treatment

Sludge was acquired from the Nasiruddin Palm Oil Mill in Bota. The sodium hydroxide (NaOH), hydrochloric acid (HCl) and methylene blue (MB) dye were acquired from Sigma-Aldrich. MB trihydrate was dissolved with deionised water to prepare a 1000 milligram per litre (mg/L) stock solution of MB, and it was then diluted into desired initial concentrations. The MB concentration was measured with UV-Vis Spectrophotometer with the wavelength set at 665 nm (Fan et al., 2017). A standard solution of MB between 20 mg/L and 220 mg/L was prepared for the calibration curve. Preliminary washing of sludge with distilled water to remove contaminations on the surfaces. The sample is then weighted before drying in the oven for 24 hours at 105 degrees Celsius (°C) to calculate the moisture content of the sludge, which is around 80 %. The dried sludge was ground using a blender and sieved into 250 µm to 500 µm and kept in air-tight containers for subsequent work.

2.2 Preparation of sludge derived biochar

The dried sludge was impregnated with sodium hydroxide (NaOH) solution with a 3:1 weight ratio of sludge to NaOH with a magnetic stirrer before placing in the oven for 24 hours at 105 ℃ for the drying process. Then, the dried impregnated sludge underwent pyrolysis process in a tube furnace under a nitrogen atmosphere with a heating rate of 10 degrees Celsius per minute (^{0}C/min) for 2 hours at 750 ℃ to produce sludge derived biochar (SB). The mass of SB was measured after the pyrolysis process. SB was washed with deionised water and diluted sulphuric acid (H_2SO_4) solution until the effluent reaches the neutral pH between 6 and 8. The sample was then filtered and dried in the oven for 24 hours at 105 ℃. Finally, the sample is stored in an air-tight container before further work. The physical and chemical features of raw sludge and SB were analysed using Surface Area and Porosity (SAP) Analyser, Field Emission Scanning Electron Microscopy (FESEM). The textural property of SB was analysed by SAP analyser. The BET multipoint was used to calculate the surface area of the SB. The surface morphology and element distribution were determined by using FESEM.

2.3 Adsorption studies

Adsorbent dosages of 0.5 g and 1 g with a contact time of 45 minutes and 60 minutes for the adsorption process were investigated in this study. The adsorbent at different doses was added to the 250 mL conical flask with 50 millimetres (mL) of 200 mg/L MB solution and was then shaken at different contact times on the orbital shaker at 120 rpm. The solution was filtered, and the filtered adsorbents were dried at 105 ℃ for 24 hours and characterised using FESEM. Absorbance test was done on the filtrate. The nomenclature used for the adsorption studies was SB(D)-T, where D is the adsorbent dosage, and T is the contact time. The removal efficiency (R) and adsorption capacity of MB were calculated using the following formulae, respectively:

$$\mathrm{R}\ (\%) = (\mathrm{C_0} - \mathrm{C_t})/\mathrm{C_0} \times 100\% \quad (1)$$

$$\mathrm{q_t} = (\mathrm{C_0} - \mathrm{C_t}) \times (\mathrm{V/m}) \quad (2)$$

where, q_t is the amount of MB adsorbed at time, t (mg/g), C_0 and C_t is the concentration of MB solution at initial and at time, t (mg/L), V is the volume of MB solution (L) and m is the mass of adsorbent (g).

2.4 Adsorption Isotherm and Kinetic

The adsorption isotherm and adsorption kinetic studies were conducted in a conical flask with 200 mL of MB solution with a varying initial concentration of 50 – 250 mg/L. The experiment was carried out with 2 g of SB adsorbent. The conical flasks were placed on the orbital shaker for 120 minutes at 150 rpm. MB samples of 10 mL were collected every 10 minutes. Langmuir and Freundlich's isotherm adsorption models were evaluated to depict the adsorption mechanism of MB. The adsorption equilibrium and kinetics are defined in the linear form shown in the Table1 (Fan et al., 2017; Ferrentino et al., 2020), where, q_m is the maximum monolayer adsorption capacity (mg/g), q_e and q_t is the amount of MB solution adsorbed at equilibrium and at time, t, respectively (mg/g), C_e and C_0 is the equilibrium and initial concentration of MB in the liquid phase, respectively (mg/L), K_L is the Langmuir adsorption constant (L/mg), K_F is the relative sorption capacity of the sorbent ((mg/g)(mg/L)$^{-1/n}$), n is the degree of dependence of sorption on the equilibrium concentration of MB, t

is the MB adsorbed at time, t (min), and k_1 (min^{-1}) and k_2 (g/mg.min) are the first-order and second-order adsorption rate constant, respectively.

Table 1: Equilibrium and kinetic equations

Models		Name
Equilibrium		
$\frac{1}{q_e} = \frac{1}{K_L q_m}\frac{1}{C_e} + \frac{1}{q_m}$	(3)	Langmuir
$\ln q_e = \ln K_F + (1/n)\ln C_e$	(4)	Freundlich
$R_L = 1/(1 + K_L C_0)$	(5)	Separation factor
Kinetic		
$\log (q_e - q_t) = \log q_e - ((k_1 t)/2.303)$	(6)	Pseudo-first-order
$\frac{t}{q_t} = \frac{1}{k_2 {q_e}^2} + \frac{1}{q_e} t$	(7)	Pseudo-second-order

3. Result and Discussions

3.1 FESEM Analysis

FESEM micrographs of raw sludge, SB, and SB after adsorption are shown in Figure 1 below. In Figure 1(a), the surface of raw sludge had a smooth surface with small pores. An adsorbent with bigger pore size has a good adsorption capacity (Kutty et al., 2019). As a result of the channels from the pores and voids to the active sites in the internal pores of the sludge, an improvement in the MB molecules' adsorption was observed in this study (Ahmed et al., 2019). The surface of SB in Figure 1(b) has a more homogeneous structure, with semi-spherical forms and no apparent pores. However, there might be a possibility of a large porous structure. The surface of SB became a bit rougher because of the adsorption of MB molecules onto the adsorbent surface, as shown in Figure 1(c).

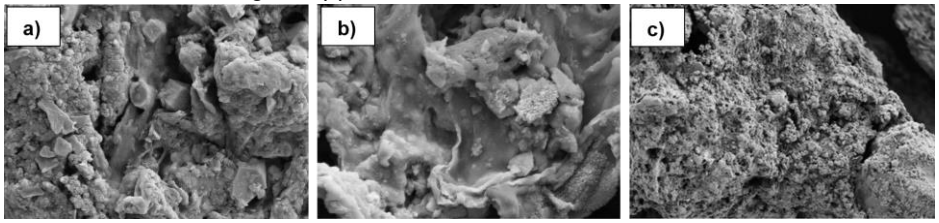

Figure 1: FESEM Micrographs of (a) raw sludge; (b) SB; (c) SB after adsorption

3.2 SAP Analysis

The pore structure of raw sludge and SB was analysed with an SAP analyser. Figures 2(a) and 2(b) exhibit type IV isotherms according to the IUPAC classification with hydrogen hysteresis loops, indicating favourable adsorption on mesoporous solids. Moreover, the high volume of nitrogen adsorbed shows high proportions of mesoporous (Ahmed et al., 2019), which suggests that the textural characteristics of the adsorbent have improved. The BET and Langmuir surface area of SB is higher than raw sludge at 25.28 m^2/g and 36.84 m^2/g, respectively. The presence of alkaline salts and other mineral elements is shown to increase the surface area, which contributes to simultaneous thermal and chemical activation during pyrolysis (Ahmed et al., 2019). The Barrett-Joyner-Halenda (BJH) method was used to determine pore size and volume. The pore volume of SB increases to 0.034 cm^3/g, but the pore size has decreased from 42.91 nm to 29.29 nm. The pores indicate that SB is mesoporous, which leads to high MB adsorption with minimal resistance to diffusion (Ahmed et al., 2019). Organics of carbon-based materials stimulated higher adsorption from high porosity and large pore volume with a pore-filling effect (Ahmed et al., 2019).

3.3 Effect of contact time and adsorbent dose on adsorption of MB

The performance of MB adsorption was studied using adsorbent dosage of 0.5 g and 1 g with a contact time of 45 minutes and 60 minutes. Equation (1) and Equation (2) are used to evaluate the removal efficiency and adsorption capacity, respectively. According to Figure 3, as the adsorbent dose and contact time increases, the removal efficiency also increases. The increase in the binding sites for adsorption enhances the adsorption rate, which increases the removal efficiency (Fan et al., 2017). However, the adsorption capacity decreases as the adsorbent dose increases. The decrease in adsorption capacity might be due to adsorbate saturation from the decrease in the adsorption active sites or the increase in the adsorbent surface area,

which decreases the number of MB molecules per unit of adsorbent. The highest adsorption capacity of 15.37 mg/g is achieved with SB (0.5)-60. However, some studies indicate that when the adsorbent dosage further increases, the removal rate and adsorption capacity become stagnant due to MB molecule saturation in the adsorption sites (Fan et al., 2017). As the contact time increases, the adsorption capacity and removal efficiency of MB from the aqueous solution increases. However, as the adsorbent dosage for adsorption of MB increases, the adsorption capacity decreases while the removal percentage increases.

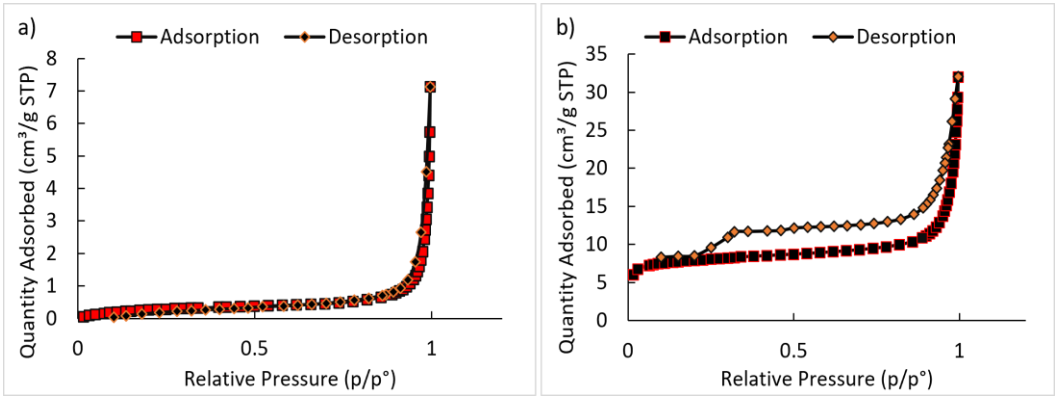

Figure 2: Adsorption-desorption isotherms of: (a) raw sludge; (b) SB

Table 2: Porous textural parameters analysis of raw sludge and SB

Material	Raw sludge	SB
BET surface area (m^2/g)	1.10	25.28
Pore volume (cm^3/g)	0.0108	0.0340
Pore size (nm)	42.91	29.29

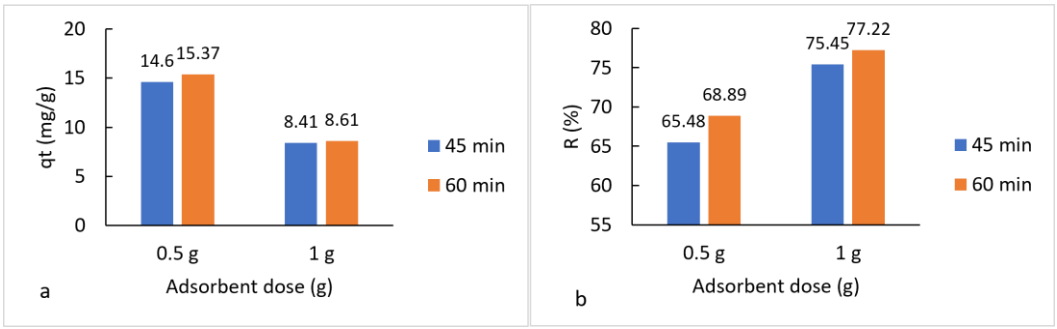

Figure 3: Adsorbent dosage and contact time effect of MB: (a) adsorption capacity, (b) removal efficiency

3.4 Adsorption Isotherms

A different range of MB concentration (50 mg/L – 250mg/L) was used to carry out the isotherm study of SB on MB solution. The Langmuir and Freundlich isotherm models were used to fit the adsorption equilibrium data for SB using Equation (3) and Equation (4), respectively, and the respective parameters and correlation are reported in Table 3. The Langmuir model fit the data better than the Freundlich model with a correlation coefficient (R^2) of 0.9895, implying monolayer adsorption and a homogeneous surface of MB onto SB (Ferrentino et al., 2020). The value of R_L obtained is greater than zero and less than one, which suggests that it is favourable adsorption (Fan et al., 2017). The R^2 shown on these models showed a strong affinity for the adsorption of MB onto SB.

Table 3: The parameters of Langmuir and Freundlich adsorption isotherm

Langmuir				Freundlich		
q_m (mg/g)	K_L (L/mg)	R^2	R_L	n	K_F	R^2
2.023	0.629	0.9895	0.0063	7.446	1.199	0.9288

3.5 Adsorption Kinetics

Equation (2) was used to calculate the adsorption capacity of MB at equilibrium. Figure 4 demonstrates that as the MB concentration increases, the adsorption capacity also increases. The increase in MB molecules for adsorption or increased interaction between adsorbent and MB molecules due to higher mass transfer driving force causes the increase in the adsorption capacity (Nasrullah et al., 2018). The adsorption capacity exhibits a drastic increase, and then it plateaus as it reaches equilibrium around 30 – 70 minutes into the adsorption process. Based on Table 4, the R^2 for pseudo-first-order kinetics was between 0.0281 to 0.6053 for all concentrations ranges, and the calculated q_e does not match the experimental q_e values. Conversely, the experimental data were well fitted with pseudo-second-order kinetics with an R^2 higher than 0.9994 and closer to unity. Based on the assumption that chemisorption involving valency forces may be the rate-limiting step through electron exchanging and sharing, pseudo-second-order kinetics is likely to describe the system in this study (Chaukura et al., 2017).

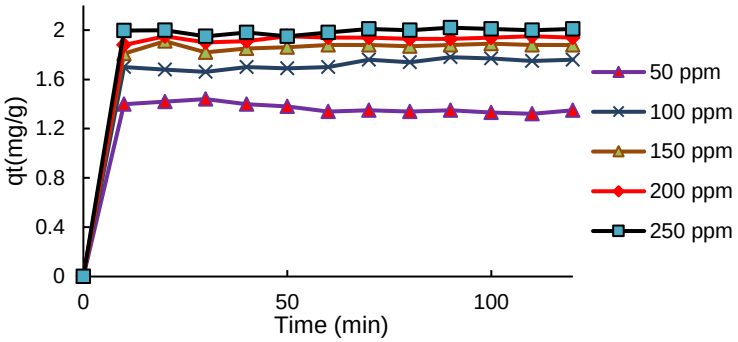

Figure 4: Kinetic curves for MB adsorption onto SB

Table 4: Parameters of pseudo-first-order and pseudo-second-order kinetic model

C_0 (mg/L)	$q_{e,exp}$ (mg/g)	Pseudo-first-order			Pseudo-second-order		
		$q_{e,cal}$ (mg/g)	K_1 (min^{-1})	R^2	$q_{e,cal}$ (mg/g)	K_2 (min^{-1})	R^2
50	1.35	0.1466	0.0051	0.0281	1.3245	-0.6377	0.9995
100	1.76	0.2729	0.0207	0.3002	1.7759	0.4642	0.9994
150	1.88	0.3797	0.0281	0.6053	1.8871	1.3631	0.9999
200	1.94	0.3167	0.0251	0.2231	1.9451	1.8838	0.9999
250	2.01	0.1244	0.0170	0.1557	2.0145	1.0058	0.9998

4. Conclusions

This study has achieved the main objective which is to study the effect of activating agents NaOH on SB biochar where SB had mesoporous pores with a surface area of 25.28 m2/g and pore volume of 0.0340 cm^3/g. The batch adsorption experiment shows a promising result in which the highest adsorption capacity of MB obtained was 2.0235 mg/g mg/g at 60 min contact time,250 mg/L initial MB concentration, and 1 g adsorbent dosage. The results show that the adsorption via the pseudo-second-order kinetic model and Langmuir isotherm model was best suited for MB removal compared to Pseudo-first-order and Freundlich model.

Acknowledgments

The authors would like to thank Universiti Teknologi PETRONAS (UTP) Malaysia for funding the project through the Yayasan Universiti Teknologi PETRONAS (YUTP) with grant code YUTP-015LC0-210.

References

Ahmad, M.A., Ahmad, N. and Bello, O.S., 2015. Modified durian seed as adsorbent for the removal of methyl red dye from aqueous solutions, Applied Water Science, 5(4), 407-423.

Ahmed, M.J., Okoye, P.U., Hummadi, E.H. and Hameed, B.H., 2019, High-performance porous biochar from the pyrolysis of natural and renewable seaweed (Gelidiella acerosa) and its application for the adsorption of methylene blue, Bioresource technology, 278, 159-164.

Chaukura, N., Murimba, E.C. and Gwenzi, W., 2017,Sorptive removal of methylene blue from simulated wastewater using biochars derived from pulp and paper sludge, Environmental Technology & Innovation, 8, 132-140.

Ding, Z., Wan, Y., Hu, X., Wang, S., Zimmerman, A.R. and Gao, B., 2016, Sorption of lead and methylene blue onto hickory biochars from different pyrolysis temperatures: importance of physicochemical properties, Journal of Industrial and Engineering Chemistry, 37, 261-267.

Fan, S., Wang, Y., Wang, Z., Tang, J., Tang, J. and Li, X., 2017, Removal of methylene blue from aqueous solution by sewage sludge-derived biochar: Adsorption kinetics, equilibrium, thermodynamics and mechanism, Journal of Environmental Chemical Engineering, 5(1), 601-611.

Ferrentino, R., Ceccato, R., Marchetti, V., Andreottola, G. and Fiori, L., 2020, Sewage sludge hydrochar: an option for removal of methylene blue from wastewater, Applied Sciences, 10(10), 3445.

Guo, H., Bi, C., Zeng, C., Ma, W., Yan, L., Li, K. and Wei, K., 2018, Camellia oleifera seed shell carbon as an efficient renewable bio-adsorbent for the adsorption removal of hexavalent chromium and methylene blue from aqueous solution, Journal of molecular liquids, 249, 629-636.

Hezam Saeed, A.A., Harun, N.Y., Sufian, S. and Bin Aznan, M.F., 2020, Effect of Adsorption Parameter on the Removal of Nickel (II) by Low-Cost Adsorbent Extracted From Corn Cob, International Journal of Advanced Research in Engineering and Technology (IJARET), 11(9).

Kutty, S.R.M., Almahbashi, N.M.Y., Nazrin, A.A.M., Malek, M.A., Noor, A., Baloo, L. and Ghaleb, A.A.S., 2019, Adsorption kinetics of colour removal from palm oil mill effluent using wastewater sludge carbon in column studies, Heliyon, 5(10), 02439.

Paranavithana, G.N., Kawamoto, K., Inoue, Y., Saito, T., Vithanage, M., Kalpage, C.S. and Herath, G.B.B., 2016, Adsorption of Cd 2+ and Pb 2+ onto coconut shell biochar and biochar-mixed soil, Environmental Earth Sciences, 75(6), 484.

Lian, F., Cui, G., Liu, Z., Duo, L., Zhang, G. and Xing, B., 2016, One-step synthesis of a novel N-doped microporous biochar derived from crop straws with high dye adsorption capacity, Journal of Environmental Management, 176, 61-68.

Mashkoor, F.and Nasar, A.,2020, Magnetized Tectona grandis sawdust as a novel adsorbent: preparation, characterization, and utilization for the removal of methylene blue from aqueous solution, Cellulose, 27(5), 2613-2635.

Nasrullah, A., Bhat, A.H., Naeem, A., Isa, M.H. and Danish, M., 2018, High surface area mesoporous activated carbon-alginate beads for efficient removal of methylene blue, International journal of biological macromolecules, 107, 1792-1799.

Otero, M., Rozada, F., Calvo, L.F., Garcıa, A.I. and Moran, A., 2003, Kinetic and equilibrium modelling of the methylene blue removal from solution by adsorbent materials produced from sewage sludges, Biochemical Engineering Journal, 15(1), 59-68.

Saeed, A.A.H., Saimon, N.N., Ali, M.W., Kidam, K., Jusoh, Y.M., Jusoh, M. and Zakaria, Z.Y., 2018, Effect of particle size on the explosive characteristics of grain (Wheat) starch in a closed cylindrical vessel, Chemical Engineering Transactions, 63, 571-576.

Saeed, A.A.H., Harun, N.Y., Sufian, S., Bilad, M.R., Nufida, B.A., Ismail, N.M., Zakaria, Z.Y., Jagaba, A.H., Ghaleb, A.A.S. and Al-Dhawi, B.N.S., 2021a, Modeling and optimization of biochar based adsorbent derived from Kenaf using response surface methodology on adsorption of Cd2+. Water, 13(7), 999.

Saeed, A.A.H., Harun, N.Y., Nasef, M.M., Al-Fakih, A., Ghaleb, A.A.S. and Afolabi, H.K., 2021b, Removal of cadmium from aqueous solution by optimized rice husk biochar using response surface methodology, Ain Shams Engineering Journal.

Saeed, A.A.H., Harun, N.Y. and Nasef, M.M., 2019, Physicochemical characterization of different agricultural residues in malaysia for bio char production, International Journal of Civil Engineering and Technology (IJCIET), 10(10), 213-225.

Saeed, A.A.H., Harun, N.Y., Sufian, S., Siyal, A.A., Zulfiqar, M., Bilad, M.R., Vagananthan, A., Al-Fakih, A., Ghaleb, A.A.S. and Almahbashi, N., 2020, Eucheuma cottonii Seaweed-Based Biochar for Adsorption of Methylene Blue Dye, Sustainability, 12(24), 10318.

Sajab, M.S., Chia, C.H., Zakaria, S., Jani, S.M., Khiew, P.S. and Chiu, W.S., 2010, Removal of copper (II) ions from aqueous solution using alkali-treated kenaf core fibres, Adsorption Science & Technology, 28(4), 377-386.

Tripathi, M., Sahu, J.N. and Ganesan, P., 2016, Effect of process parameters on production of biochar from biomass waste through pyrolysis: A review, Renewable and Sustainable Energy Reviews, 55, 467-481.

Vithanage, M., Mayakaduwa, S.S., Herath, I., Ok, Y.S. and Mohan, D., 2016, Kinetics, thermodynamics and mechanistic studies of carbofuran removal using biochars from tea waste and rice husks, Chemosphere, 150, 781-789.